PHOTONICS Research

Laser fabrication of graphene-based supercapacitors

Xiu-Yan Fu,[1] Zhao-Di Chen,[1] Dong-Dong Han,[1,3] Yong-Lai Zhang,[1,4] Hong Xia,[1] and Hong-Bo Sun[2]

[1]State Key Laboratory of Integrated Optoelectronics, College of Electronic Science and Engineering, Jilin University, Changchun 130012, China
[2]State Key Laboratory of Precision Measurement Technology and Instruments, Department of Precision Instrument, Tsinghua University, Beijing 100084, China
[3]e-mail: handongdong@jlu.edu.cn
[4]e-mail: yonglaizhang@jlu.edu.cn

Received 15 November 2019; revised 8 January 2020; accepted 30 January 2020; posted 31 January 2020 (Doc. ID 382401); published 1 April 2020

Supercapacitors (SCs) have broad applications in wearable electronics (e.g., e-skin, robots). Recently, graphene-based supercapacitors (G-SCs) have attracted extensive attention for their excellent flexibility and electrochemical performance. Laser fabrication of G-SCs exhibits obvious superiority because of the simple procedures and integration compatibility with future electronics. Here, we comprehensively summarize the state-of-the-art advancements in laser-assisted preparation of G-SCs, including working mechanisms, fabrication procedures, and unique characteristics. In the working mechanism section, electric double-layer capacitors and pseudocapacitors are introduced. The latest advancements in this field are comprehensively summarized, including laser reduction of graphene oxides, laser treatment of graphene prepared from chemical vapor deposition, and laser-induced graphene. In addition, the unique characteristics of laser-enabled G-SCs, such as structured graphene, graphene hybrids, and heteroatom doping graphene-related electrodes, are presented. Subsequently, laser-enabled miniaturized, stretchable, and integrated G-SCs are also discussed. It is anticipated that laser fabrication of G-SCs holds great promise for developing future energy storage devices.

https://doi.org/10.1364/PRJ.382401

1. INTRODUCTION

Energy storage devices play important roles in smart electronics, such as e-skin [1–4], sensors [5,6], wearable units [7–11], and other applications [12–17]. Among various energy storage devices [18–25], supercapacitors (SCs) show obvious superiority, such as high power density, fast charge/discharge rates, and high cycle stability [26–30]. Typically, the device structure of an SC contains electrolytes and electrode materials [31–36]. Generally, electrolytes and electrode materials are assembled in a plane or sandwich structure. During charging and discharging processes of SCs, physical adsorption/desorption of electrolyte ions or a reversible redox reaction occurs on the electrode–electrolyte interface [37–40]. Nowadays, in order to improve SC performance, more and more effective materials have been developed to design and fabricate high-performance electrode materials [41,42].

From the point of view of materials, graphene has high mechanical flexibility, strength, electrical conductivity, and surface area [43–47]. Because of these excellent properties, graphene plays an important role in satisfying the requirements for high-performance electrode materials. In addition, graphene-based supercapacitors (G-SCs) are able to act as flexible and deformable energy storage devices in electronic skins, wearable displays, curved smartphones, etc. [48–50]. Initially, graphene was prepared by mechanical exfoliation. This kind of graphene shows ultrahigh conductivity; however, graphene prepared by mechanical exfoliation suffers from small size and irregular shape, which is not suitable for fabricating SC electrodes. In recent years, technological advances have been made in large-area graphene film preparation, such as reduction of graphene oxide (RGO) [51,52] and chemical vapor deposition growth graphene (CVDG) [53]. Therefore, tremendous preparation methods involving chemicals, high-temperature treatment, etc., have been investigated to fabricate G-SCs. Recently, laser technologies have been adopted: laser reduction of graphene oxides (LRGOs), laser treatment of CVDGs (LCVDGs), and laser-induced graphene (LIG) [54]. Compared with the graphene prepared via mechanical exfoliation, thermal/chemical RGO and CVDG, laser-enabled graphene can be prepared in large-area films with high electrical conductivity, flexibility, and high chemical/physical stability. Importantly, compared with these fabricating methods, laser is a powerful tool to fabricate G-SCs, which avoids the need for

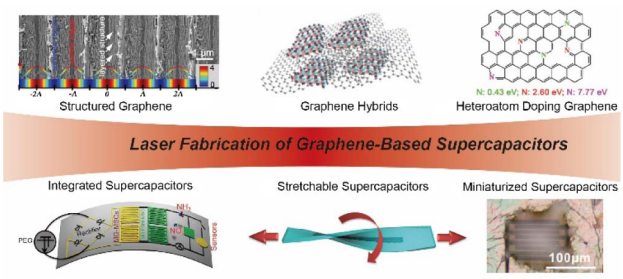

Fig. 1. Progress in laser fabrication of G-SCs. The structured graphene image, adapted from Ref. [56]; the graphene hybrid image, adapted from Ref. [57]; heteroatom doping graphene image, adapted from Ref. [58]; the miniaturized SC image, adapted from Ref. [59]; the stretchable SC image, adapted from Ref. [60]; the integrated SC image, adapted from Ref. [61].

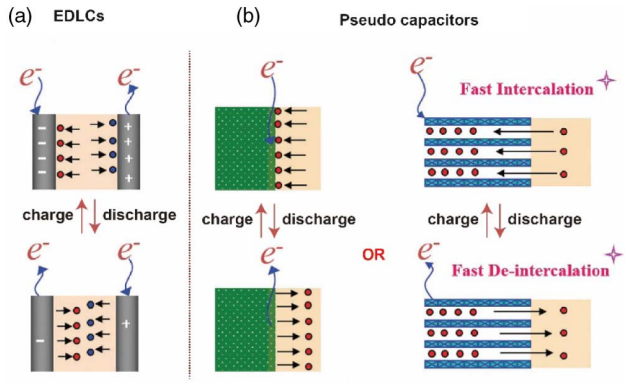

Fig. 2. Working mechanism of SCs including (a) EDLCs and (b) pseudo-capacitors; adapted from Ref. [62].

additional toxic-reducing agents, high temperature, and inert gas protection. Also, laser technologies allow high resolution for miniaturized SC design and fabrication. Moreover, laser technologies permit programmable patterning in arbitrary shapes and are also compatible with other functional units for integration [55]. Therefore, laser fabrication of G-SCs holds great potential for effective energy storage devices.

In this review, we summarize the advancements in laser-assisted preparation of G-SCs (Fig. 1). First, in the working mechanism section, electric double-layer capacitors (EDLCs) and pseudo-capacitors are introduced. Second, laser fabrication of G-SCs has been reviewed, including LRGO-SCs, LCVDG-SCs, and LIG-SCs. Third, a brief summary of unique characteristics of laser-enabled G-SCs, including ease of developing structured, hybrid, heteroatom doping-based graphene electrode materials, miniaturized SCs, stretchable SCs, and integrated SCs, is discussed. Finally, future perspectives are highlighted.

2. LASER FABRICATION OF GRAPHENE-BASED SCs

In this section, we summarize the working mechanism of SCs, including EDLCs and pseudo-capacitors and review laser-enabled fabrication of G-SCs, including LRGO-SCs, LCVDG-SCs, and LIG-SCs.

A. Working Mechanism of SCs

The working mechanism of laser fabrication of G-SCs is divided into two types: EDLCs and pseudo-capacitors [62–64].

As for EDLCs [Fig. 2(a)], physical adsorption/desorption of electrolyte ions occurs on the interface of the electrode–electrolyte during the charge/discharge process. Benefiting from rapid physical adsorption/desorption, EDLCs usually exhibit short charging time, high power density, and long cycle lives. However, capacitance values of EDLCs are low due to the limited effective surfaces of electrode materials. Laser-enabled graphene acts as an electrode material because the excellent conductivity, chemical stability, and high surface area of graphene contributes to formatting EDLCs.

As shown in Fig. 2(b), the working mechanism of pseudo-capacitors is decided by a fast reversible Faradic process at the electrode–electrolyte interface. The fast reversible Faradic process also occurs near the surface of active electrode materials. Importantly, due to Faradic processes, pseudo-capacitors have higher pseudo-capacitance. Nevertheless, the existing of pseudo-capacitive materials suffers from lower power density because of the poor conductivity during redox processes, and redox reactions will reduce cycle lives during charging and discharging processes. At present, the most widely explored pseudo-capacitive materials include transition metal oxides or hydroxides, conducting polymers, and materials possessing surface functional groups. Recently, laser-enabled graphene hybrids and heteroatom doping graphene have been developed as pseudo-capacitive materials. In addition, laser-enabled graphene has porous or grating structures, which helps with intercalation and deintercalation.

B. LRGO-Based SCs

Graphene oxide (GO) is an important derivative of graphene, which bears plenty of oxygen-containing groups (OCGs) on the plane of graphene [65,66]. In general, due to existing OCGs, GO film is electric insulation and has low surface area. In order to remove the OCGs, thermal methods (>1000°C) and chemical methods have been widely used for producing graphene-related materials. After thermal and chemical processes, the obtained RGO usually possesses high conductivity, and the obtained devices show excellent electrochemical performance.

Increasingly, as shown in Fig. 3(a), OCGs can be removed via the photoreduction method [67]. After photoreduction processes, the resulted RGO shows high electrical conductivity. Currently, various light sources have been adopted for GO photoreduction, such as UV light [68,69], flash [70], and even sunlight [71,72]. Among these light sources, laser plays an important role in mask-free programmable reduction of GO and laser carving of RGO. As for the LRGO, laser reduction mainly undergoes photothermal reduction ($\lambda > 390$ nm) or photochemical reduction ($\lambda < 390$ nm) processes, which depends on the wavelength of the laser [73]. Compared with thermal/chemical reduction routes, LRGO can be prepared with similar conductivity and surface area by tuning the processed laser beam power, scanning speed, scanning step length, and exposure duration [74–77]. In addition, laser reduction shows unique advantages in any designable patterning, hierarchical

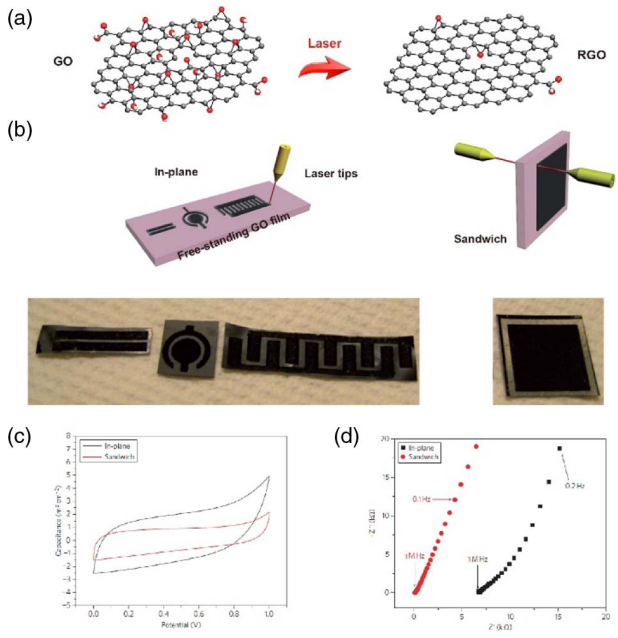

Fig. 3. (a) Schematic illustration of LRGO, adapted from Ref. [67]; (b) schematics and photos of planar and sandwiched LRGO electrodes on GO paper; (c) CV plots of planar and sandwich SCs (scan rate, 40 mV/s); (d) impedance spectra for the in-plane and sandwich devices; (b)–(d) adapted from Ref. [87].

structuring, heteroatom doping, device miniaturization, and device integration.

As a typical example, Zhang *et al.* successfully achieved LRGO [78]. Specifically, a femtosecond laser was used to reduce and pattern LRGOs with high resolutions (~500 nm). In this manner, any desired RGO patterns were successfully fabricated, such as graphene microcircuits and spiderwebs [58]. Subsequently, various laser devices were used to reduce and pattern GOs, such as UV lasers, CO_2 lasers, and infrared lasers [79–86]. As a benefit from any designable patterning, LRGOs can be used to design SC electrodes. For example, Gao *et al.* patterned both planar and sandwiched LRGO electrodes on GO paper [Fig. 3(b)] [87]. In this case, GO film with trapped water served as both solid electrolyte and separator because of the ionic conductivity and electrical insulation. After laser reduction, the LRGO region turned to black due to the deoxydation process. It is worth noting that the obtained in-plane SC delivers the highest specific capacitance of ~0.51 $mF \cdot cm^{-2}$ [Figs. 3(c) and 3(d)]. This work provides a very easy and useful device structure for LRGO-SCs. A similar design for electrolytes was reported based on LRGO/polyvinyl alcohol-GO/LRGO (LRGO/PVA-GO/LRGO) [88]. In addition, Qu *et al.* successfully achieved RGO–GO–RGO fiber SCs [89]. This fiber SC has wide prospects for wovening. Additionally, to satisfy the increasing demand for on-chip energy storage, Kaner and El-Kady used a LightScribe DVD burner to fabricate graphene microsupercapacitors (MSCs) to scale. Over 100 MSCs can be fabricated in 30 min or less [90]. Notably, These MSCs exhibit the highest power density of ~200 $W \cdot cm^{-3}$.

Laser carving is capable of being applied on RGO-based materials. Different from laser reduction and patterning, after laser carving processes, unwanted RGOs were removed [91–93]. For example, Wong *et al.* achieved MSCs via laser patterning and ablation [94]. First, the laser beam was used to pattern and reduce the GO films; after that, the laser beam with high power was applied to ablate the unwanted area. It is worth noting that this work overcomes the size/performance limitations for current MSCs and exhibits overwhelming volumetric energy density compared with commercial MSCs, even at a 1000 mV/s scan rate. Alternatively, due to the limited electrical conductivity of conventional LRGOs, Shi *et al.* laser-carved a low sheet resistance (1.28 $\Omega \cdot sq^{-1}$) and mechanically robust (330 MPa) RGO film [91]. After the laser carving process, the electrodes were shaped into designed in-plane structures. The devices achieved a high areal specific capacitance of 15.38 $mF \cdot cm^{-2}$. These methods hold promise for improving the performance of RGO-SCs.

C. LCVDG-Based SCs

Although GO can be reduced to recover conductivity by laser technologies, LRGO suffers from limited electrical conductivity. To produce graphene with high conductivity, CVDG is considered as an effective method for developing high-quality graphene. Typically, Cu or Ni foils under a gas mixture of CH_4 and H_2 are used as a catalytic substrate for graphene growth [95–100]. In order to obtain high-quality CVDGs, the gas ratio of CH_4:H_2, growth time, and cooling rate need to be optimized. Nevertheless, CVDG needs to be transferred to target substrates for use and suffers low production.

Typically, Zhu *et al.* used the direct laser writing (DLW) technology to achieve multilayered graphene-based MSCs (MG-MSCs) [59]. The high power of laser beam enables removal of CVDG. This process is able to pattern CVDG and yet retain the high conductivity of CVDG. As shown in Fig. 4(a), direct ultraviolet laser machining is applied to multilayered graphene (MG) to obtain interdigital microelectrodes. The DLW technique applied in this work plays an important role in highly efficient preparation. The as-fabricated MG-MSCs possess high areal and volumetric capacitances of 62.7 $\mu F \cdot cm^{-2}$ [Figs. 4(b) and 4(c)]. The device performance may be improved by optimizing the thickness of the MG.

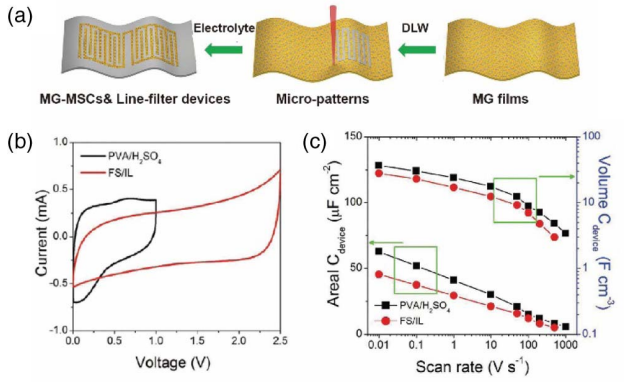

Fig. 4. (a) Scheme for the preparation of graphene-based microsupercapacitors (G-MSCs); (b) CV curves of G-MSCs on PET substrates and (c) corresponding areal and volumetric capacitances at different scan rates; adapted from Ref. [59].

In addition, a sequential transfer process is another key process in fabricating MG-MSCs.

D. LIG-Based SCs

Recently, various studies have demonstrated that LIG is another scalable approach for producing graphene. The LIG process is defined as laser graphitization in polymers. The structural features of polymers, including aromatic and imide repeat units, play an important role in LIG. As shown in Fig. 5(a), Tour *et al.* successfully prepared LIG from polyimide (PI) [101]. In their work, a CO_2 infrared laser was applied to accomplish the thermal conversion. As shown in Fig. 5(b), LIG has been developed to pattern into an owl shape. Specifically, the 2D peak of LIG (centered at 2700 cm^{-1}) is similar to single-layer graphene [Fig. 5(c)]. The X-ray diffraction (XRD) pattern of LIG displays an intense peak (centered at 25.9°), which indicates an interlayer spacing of ~3.4 Å [Fig. 5(d)]. The resulting LIG shows high electrical conductivity. The laser-patterned interdigital electrodes for in-plane MSCs exhibit excellent performance (>4 $mF \cdot cm^{-2}$) that is comparable to RGO-SCs. What is more, this technology is able to fabricate vertically stacked SCs for practical application [102].

Particularly, based on the similar preparation mechanism, LIG process has been extended using diverse materials such as wood [103], food, cloth, and paper [104]. Recently, Lamberti *et al.* demonstrated an all-sulfonated poly(ether ketone) (SPEEK) flexible SC, in which SPEEK served as both separator and polymeric electrolyte [105]. The graphitization mechanism of SPEEK can be summarized as laser-induced reticulation, during which sulfonic groups degrade and oxidatively dehydrogenate.

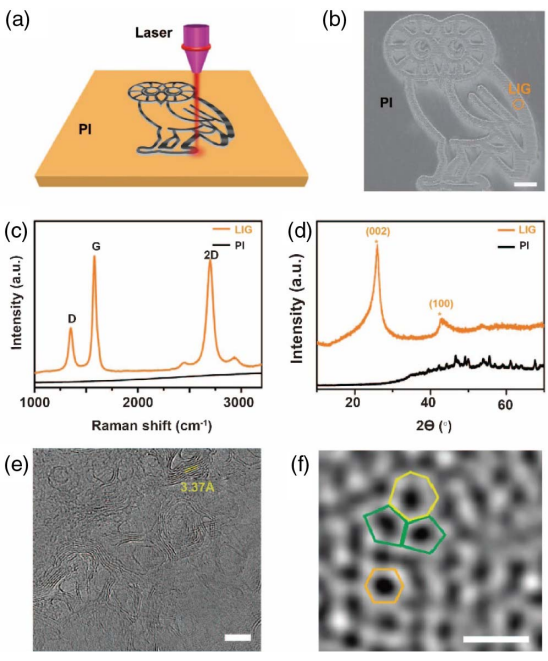

Fig. 5. (a) Diagram of LIG converted from PI; (b) scanning electron microscope (SEM) image of the as-prepared owl-shaped LIG pattern; scale bar, 1 mm; (c) Raman spectra and (d) XRD patterns of LIG and PI; (e) high-resolution transmission electron microscope (HRTEM) image of LIG; scale bar, 5 nm; (f) transmission electron microscope (TEM) image of selected area of LIG, scale bar, 5 Å; adapted from Ref. [101].

Importantly, in this work, they demonstrated that only one material was used for the whole device.

3. UNIQUE CHARACTERISTICS OF LASER-ENABLED G-SCs

In this section, the unique characteristics of laser-enabled G-SCs are summarized, including the ease of developing structured graphene and graphene hybrids, heteroatom doping of graphene-based electrode materials, and fabricating miniaturized, stretchable, integrated SCs.

A. Structured Graphene-Based Electrode Materials

Currently, to improve the surface area of graphene-based electrodes and the contact area between electrode and electrolyte, two kinds of structured graphene-based electrode materials have been well studied, including porous structures and grating structures. The porous structures are attributed to LRGO- or LIG-based electrode materials because of the gas generation during laser processing, whereas grating structures are mainly based on LRGO via the laser holography technique.

As typical examples, El-Kady *et al.* fabricated LRGO with porous structure via a laser in DVD drives [106]. During the laser reduction process, OCGs escaped from the GO nanosheets in the form of CO, CO_2, and H_2O. Because of the gas generation along with the deoxydation process, the obtained LRGO possesses a porous structure compared with the GO region layered structure. Therefore, LRGO possesses large accessible specific surface area [Brunauer–Emmett–Teller (BET) surface area: 1520 m^2/g]. The large accessible specific surface area is beneficial for avoiding the restacking of GO during the laser reduction process. Figure 6(a) shows the preparation process of LRGO-SCs. The resultant LRGO electrochemical capacitors with sandwich structure exhibit both ultrahigh energy density (1.36 $mW \cdot h/cm^3$) and power density (~20 W/cm^3). Nevertheless, the formation of porous structures is generally uncontrollable. In this regard, Zhang *et al.* reported synchronous photoreduction and hierarchical structuring of GO by using two-beam laser interference (TBLI) technologies [56]. As shown in Fig. 6(b), a laser beam is first split into two equal-intensity beams, and then the acquired two beams are guided to interfere on the surface of GO films. As a result, periodic grating structures are created by the interfered laser beams. The TBLI technology is feasible for controlling chemical composition, conductivity, microscale gratings, and layered nanoporous structures of the LRGO electrodes [Figs. 6(c) and 6(d)]. Importantly, the resultant LRGO-SCs show better electrochemical performance compared to those based on RGO without micronanostructures with the same reduction level [107].

B. Graphene Hybrid-Based Electrode Materials

Though graphene shows great superiority in developing high-performance SCs, the insufficient capacity of pristine graphene and graphene analogues-based SCs is prominent. Therefore, various studies have been carried out to fabricate graphene-based hybrid materials for performance improvement [108–110]. The advantages of graphene hybrid-based electrode materials can be summarized as follows. (1) The introduction of active materials effectively prevents the restacking of

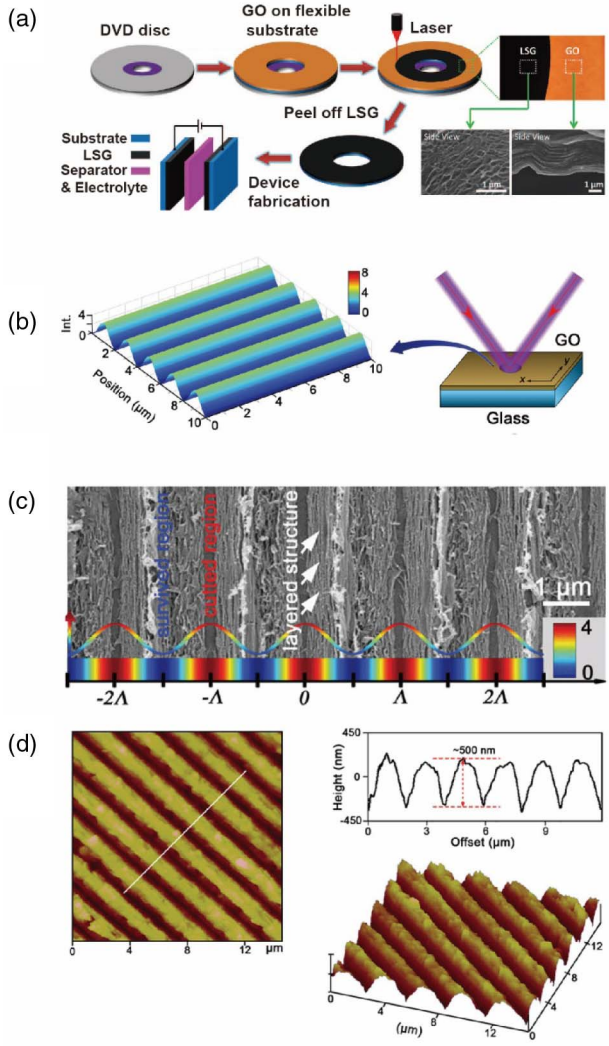

Fig. 6. (a) Diagram of LSG-based electrochemical capacitors, adapted from Ref. [106]; (b) schematic illustration of fabricating LRGO films with 1D grating structures by the TBLI technique; (c) SEM image; (d) atomic force microscope (AFM) image of LRGO films with 1D grating-like structures; (b)–(d) adapted from Ref. [56].

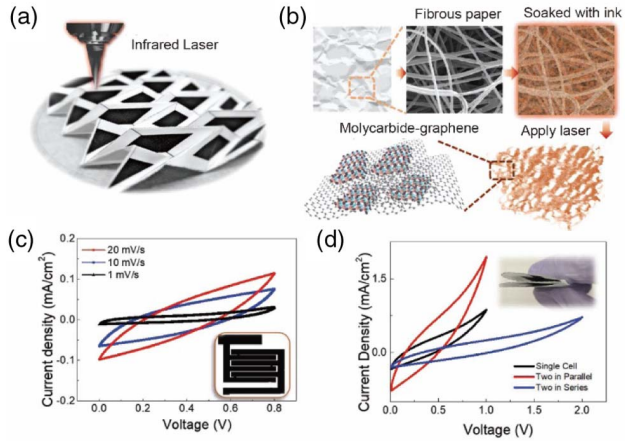

Fig. 7. (a) Photo of molybdenum carbide-graphene (MCG) fabricated by DLW on paper substrate; (b) schematic illustration of the MCG fabrication process; (c) CV curves of interdigital SC; (d) CV curves of single, parallel, and series sandwich-structure devices measured at a scan rate of 100 mV/s; adapted from Ref. [57].

graphene layers after laser reduction processes, leading to much larger specific surface areas. (2) More active sites will also be introduced to acquire higher capacity. Graphene-based hybrid materials can be fabricated by laser-reducing GO/active materials composites into LRGO-based hybrid materials, laser-induced graphene/active hybrid materials, or depositing active materials after laser reduction of GO or LIG processing [111–114].

As for laser-reducing the GO/active materials composite into the RGO-based hybrid materials, for example, Liu *et al.* successfully demonstrated LRGO/carbon nanotubes (CNTs)-MSC by laser reduction and patterning GO/CNTs hybrid powders into LRGO/CNTs MSCs [111]. In this work, CNTs were used to prevent the restacking of laser-scribed graphene layers. The CNTs are also able to improve the ion-accessible surface area. What is more, the reduction in diameter of CNTs boosts the device performance. Therefore, the device based on laser-scribed GO/single-walled carbon nanotubes (GO/SWCNTs) with a diameter of 1–2 nm exhibits the best electrochemical performance. Other works have extended the investigation by fabricating LRGO/RuO_2 [113], LRGO/Fe_3O_4 [114], and LRGO/Au nanoparticle [112] hybrid electrodes.

As for the LIG/active hybrid materials, Lamberti *et al.* have reported *in situ* MoS_2 decoration of LIG as SC electrodes [115]. In this work, the PI films were covered with a layer of MoS_2 before laser treatment. After laser writing, a material consisting of wrinkled graphene decorated by MoS_2 sheets was obtained. The resultant device shows an enhanced areal capacitance compared to that based on LIG. The improved electrochemical performance was summarized as the micro- and nano- structuralization of LIG and *in situ* decoration of MoS_2. Furthermore, Zang *et al.* fabricated hierarchically porous LIG/Mo_3C_2 samples by DLW to build paper-based 3D foldable SCs [Fig. 7(a)] [57]. In the fabrication process, gelatin-mediated inks containing Mo^{5+} ions are sprayed on paper substrates [Fig. 7(b)]. Then laser scanning is used to convert paper substrates into porous LIG/Mo_3C_2 composites. The specific capacitances are achieved: 14.0 $mF \cdot cm^{-2}$ at a scan rate of 1 $mV \cdot s^{-1}$ [Fig. 7(c)]. It is worth noting that this method enables fabrication of a single device and two devices connected in parallel/series [Fig. 7(d)].

As for depositing active materials after laser reduction of GO or LIG processing, for example, Ghoniem *et al.* used a CO_2 laser system to reduce and pattern GO [116]. After that, a Mn-oxide layer was electrodeposited on the resultant LRGO to form the hybrid electrodes. The hybrid electrodes show enhanced specific capacitance in the range of 172–368 F/g, which is much higher than that of pure LRGO electrodes (82–107 F/g). In addition, Tour *et al.* reported high-performance pseudo-capacitive MSCs from LIG, in which the laser induction process and subsequent electrodeposition of MnO_2, FeOOH, and conductive polyaniline (PANI) were used to fabricate LIG–MnO_2, LIG–FeOOH, or LIG–PANI electrodes [117].

C. Heteroatom Doping-Based Graphene Electrode Materials

Heteroatom doping has attracted much research interest in tailoring the characteristics of graphene for improving electrochemical properties because heteroatomic defects and functional groups will be introduced to graphene, leading to alteration of the electronic structure [118–124]. Compared with chemical reduction-, thermal annealing-heteroatom doping, laser-assisted heteroatom doping is a high-efficiency and chemical-free method that enables the formation of highly porous structures and operates at room temperature. Currently, various heteroatom doping methods have been adopted via solid, liquid, and gaseous state doping sources during laser reduction of GO and LIG processing.

As for the laser reduction of GO, the abundant OCGs of GO are beneficial for adjusting essential functional groups and introducing surface modification. For example, Zhang *et al.* achieved reduction and synchronous N-doping of GO based on mixtures of GO and nitrogen-rich carbon nanoparticles through DLW [125]. In this work, N content can reach ~7.78% (atomic fraction). The obtained N-doped graphene composite-based SCs deliver obvious enhanced electrochemical performance. Further study based on laser reduction of a GO/urea composite has resulted in N-doping graphene [126]. Also, as shown in Fig. 8(a), Peng *et al.* demonstrated boron-doped LIG (B-LIG) MSCs via a simple laser induction process under ambient conditions [127]. From the X-ray photoelectron spectroscopy (XPS) of B-PI and B-LIG [Fig. 8(b)], the shifting of B 1s peak indicates that boron can be attributed to B-N, BCO_2, or BC_2. Besides, atomic percentage of N drops from 7.6% to 2.0% after the laser induction process [Fig. 8(c)], showing that the reacting site is attributed to the imide group.

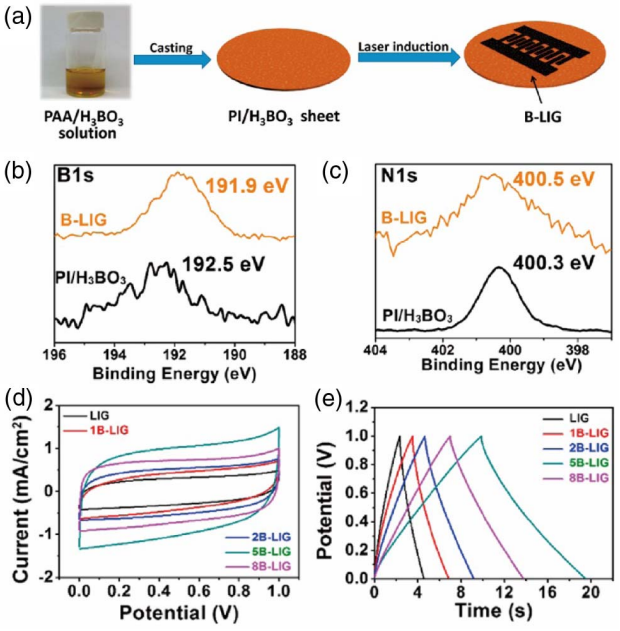

Fig. 8. (a) Illustration of the preparation of boron-doped LIG MSCs (B-LIG-MSCs); (b) B 1s spectrum and (c) N 1s spectrum of B-LIG; (d) CV curves of LIG-MSC and B-LIG-MSC; scan rate 0.1 V/s; (e) galvanostatic charge-discharge (GCD) curves of LIG-MSC and B-LIG-MSC; current density 1 mA/cm^2; adapted from Ref. [127].

Moreover, the content of H_3BO_3 is able to tune the SC performance [Figs. 8(d) and 8(e)]. Initially, the increase in H_3BO_3 improves performance because of the increasing hole charge density. In addition, higher H_3BO_3 loadings lower the formation efficiency of PI and the conductivity of the material. The resultant areal capacitance of B-LIG MSCs is 3 times higher than that based on nondoped devices.

D. Miniaturized Graphene-Based SCs

As for laser-enabled miniaturized G-SCs, there are two functions of laser technologies. One of the most obvious advantages of laser-enabled G-SCs is the miniaturization of MSCs with the resolution of micrometers [128]. Because of the high resolution, femtosecond writing technique is commonly utilized for MSC fabrication. Therefore, laser can be used to shorten diffusion paths of electron/ion between two electrodes. The other advantage is the femtosecond laser-assisted controllable microdroplet transfer technology. This technology can be used to fabricate microelectrolyte droplets on the micro SCs.

A recent work is introduced as an illustrative example. Hu *et al.* first used an *in situ* femtosecond writing technique to prepare in-plane MSCs based on LRGO/Au nanoparticles interdigitated electrodes [112]. The interdigitated electrodes are ~140 μm in width with 60 μm spacing. Thereafter, H_2SO_4/PVA hydrogel electrolyte was drop-cast onto the microelectrodes for electrochemical performance characterization. What is more, the obtained RGO/Au nanoparticles (RGO/Au NPs) MSCs exhibited superior rate capabilities. The specific capacitance retentions were 71% and 50% when the charging rate increased from 0.1 to 10 V/s and to 100 V/s, respectively. Recently, Shen *et al.* reported ultraminiature graphene MSCs by femtosecond laser DLW electrodes and controllable microdroplet transfer, as shown in Fig. 9(a) [61]. First, the femtosecond laser writing of GO (fsrGO) was 100 μm long and 8 μm wide. The interelectrode spacing was 2 μm [Fig. 9(b)]. Then, accurate transfer of electrolyte microdroplets was carried out via femtosecond laser pulses to effectively avoid the interference of electrolyte and other electronic parts, as shown in Fig. 9(c). As estimated, MSCs with interelectrode spacing of 550 μm display lower current densities than MSCs with interelectrode spacing of 2 μm. In addition, the specific capacitance of MSCs with interelectrode spacing of 2 μm is higher than that with the interelectrode spacing of 550 μm, which indicates that the miniaturization of MSC electrodes is of great benefit to increasing specific capacitance density. The corresponding cyclic voltammetry (CV) plots are shown in Figs. 9(d) and 9(e). This work highlighted the unique characteristics of the femtosecond writing technique in fabricating miniaturized electronics.

E. Stretchable Graphene-Based SCs

Currently, in order to meet the huge requirements of wearable intelligent electronic devices, stretchable G-SCs have been achieved based on laser-enabled graphene [129].

Lamberti *et al.* demonstrated a highly stretchable and flexible SC by using a polydimethylsiloxane (PDMS) substrate [60]. As shown in Fig. 10(a), first, porous LIG patterns were obtained by DLW of PI films. Then PDMS was poured onto the LIG patterns to obtain LIG/PDMS structures. Finally, a 3D LIG/PDMS SC was assembled, as shown in Fig. 10(b). Taking

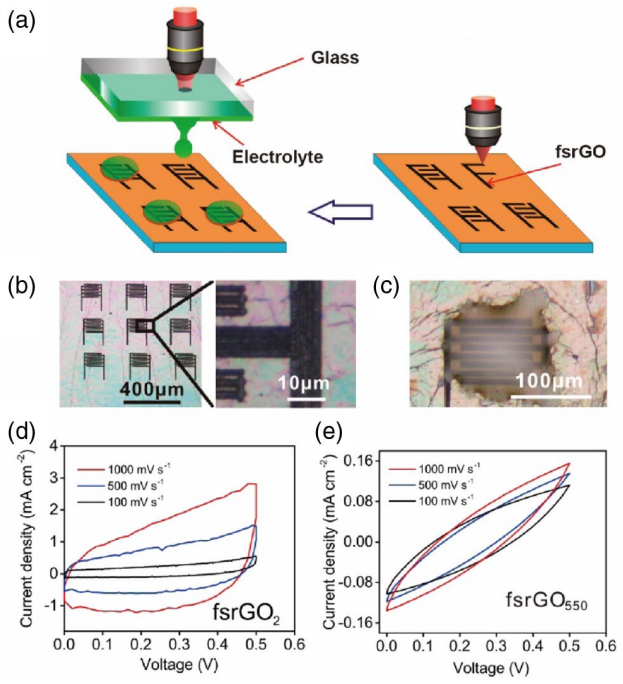

Fig. 9. (a) Fabrication process for miniaturized SCs by using a femtosecond laser; (b) RGO electrode arrays with a spacing of 2 μm; (c) optical microscope image of microelectrolyte droplets covering the electrode; CV plots of RGO MSC with interelectrode spacing of (d) 2 μm and (e) 550 μm; adapted from Ref. [61].

advantages of the mechanical property of PDMS and conductivity of LIG, the as-prepared LIG/PDMS-based SCs retained ~84% of their initial capacitance after 1000 cycles of stretching [Fig. 10(c)] and ~90% in a bending state [Fig. 10(d)]. Afterwards, Zhao *et al.* developed LRGO-GO-LRGO via region-specific reduction of GO foam [129]. Benefits from the framework, the 3D LRGO-GO-LRGO foam, show a superior electrochemical property. Importantly, the capacitance of the resulting LRGO-GO-LRGO SC can be tuned by compression situations. In addition, LRGO-GO-LRGO foam enables bending, torsion, and compression, which play important roles in stretchable electronics.

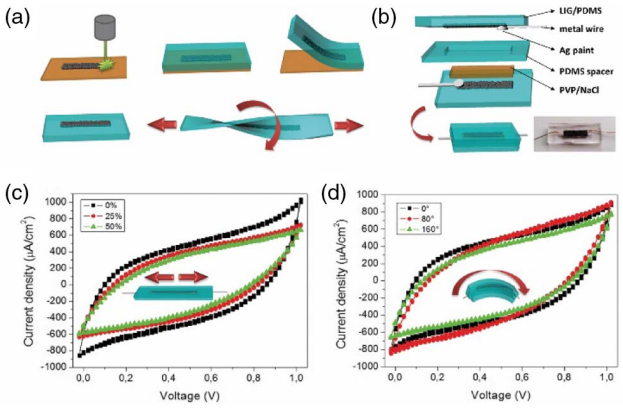

Fig. 10. (a) Schematic illustration of a highly stretchable SC using LIG electrode onto elastomeric substrate; (b) device structure; CV plots of SCs under (c) stretching and (d) bending tests; scan rate 10 V/s; adapted from Ref. [60].

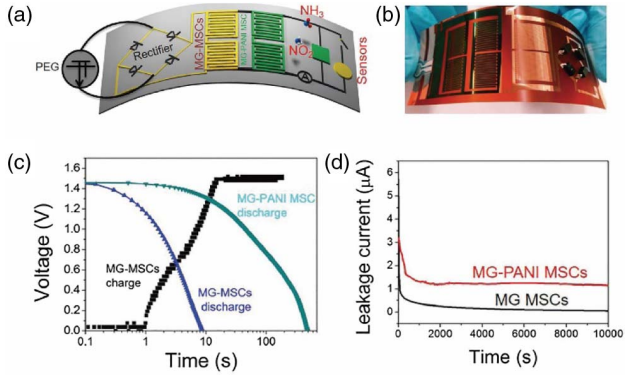

Fig. 11. (a) Illustration of an integrated device including SCs and sensors; (b) photograph of the integrated device; (c) charging and discharging curve of the MG-MSCs and discharging curves of the MG-PANI MSCs; (d) leakage currents of MSCs; adapted from Ref. [59].

F. Integrated with Other Devices

As mentioned above, laser-enabled-graphene-SCs are capable of high specific capacitance, which can be integrated with other functional devices serving as energy storage units. Importantly, laser fabrication of graphene-based electronics has broad applications in energy storage, sensors, and electrical connection. In addition, laser fabrication has been widely used in developing integrated devices, such as microcircuits [130] and energy storage devices [131]. Therefore, taking advantages of programmable writing ability, lasers have been explored in integrating G-SCs with other electronic devices. Watanabe's group reported a self-powered photodetection system by a one-step DLW of LIG [132]. The self-powered photodetection system includes an MSC and a photodetector integrated circuit, which is fabricated by one-step DLW on PI film. Then the functional modular unit was combined with a commercial solar panel to form the self-powered photodetection system. The as-prepared self-powered photodetector showed an on/off ratio of 31.2 (voltage, 0.9 V). In this work, the tightly integrated and multifunctional unit was easily prepared by the laser fabrication method. Zhu *et al.* successfully integrated G-SCs with piezoelectric generators and pressure/gas sensors [Figs. 11(a) and 11(b)] [59]. A laser beam was used to fabricate the electrode and accomplish the integration of functional units. The integrated pressure sensor is able to detect walking. Additionally, gas sensors can respond quickly to 200 ppm (parts per million) of NO_2 or NH_3 at room temperature [Figs. 11(c) and 11(d)]. In this case, the laser fabrication technique makes the integration of functional units a simplified process. In addition, G-SCs have been integrated with solar cells [133,134] and wireless devices [130]. In brief, laser fabrication shows obvious superiority in the integration of multifunctional units towards wearable and intelligent microdevices.

4. SUMMARY AND OUTLOOK

There has been much research progress since laser-enabled graphene has been successfully prepared. In this review, we

summarized the working mechanism of SCs, laser fabrication of G-SCs, and the unique characteristics of laser-enabled G-SCs.

As for the working mechanism of SCs, there are two kinds of mechanism, including EDLCs and pseudo-capacitors. Because of the high conductivity and surface area, laser-enabled graphene, including LRGO, LCVDG, and LIG, has been adopted to fabricate electrodes of SCs. Compared with the graphene prepared via mechanical exfoliation, laser-based graphene is able to prepare large-area films with high electrical conductivity, flexibility, and high chemical/physical stability. They work based on the EDLCs. Lasers also have the ability to develop doped graphene and graphene hybrids. The heteroatom doping-based graphene and graphene hybrid-based SCs can be attributed to the pseudo-capacitors.

In order to obtain high device performance, lasers have been adopted to fabricate structured graphene to improve contact area between graphene and electrolytes. Porous and grating structures have been developed for graphene. Porous structures can be fabricated by LRGO and LIG because of gas generation. The grating structures can be fabricated via laser interference. Lasers can also be used to fabricate graphene hybrids and heteroatom doping graphene for higher device performance. Graphene hybrids have been developed via laser-reduced GO composite or depositing active materials after LRGO of LIG processing. The active materials contain abundant active sites, which is helpful in improving electrochemical performance. As for doping graphene, the heteroatom doping can increase the hole charge density.

In addition to developing high electrochemical performance, lasers play an important role in developing miniaturized, stretchable, and integrated devices. Thanks to its high-resolution ability, a femtosecond laser can be used to develop miniaturized SCs. As for stretchable G-SCs, they can be fabricated for stretching substrates or stretching structures via LIG or a laser cutting process. In addition, it is worth noting that graphene is a versatile material for developing electronic devices, which are able to develop integrated SCs. For example, fabricated SCs arrays improve energy storage ability and shed light on possible practical uses.

Though many successes have been achieved in this field, there are still urgent problems to be solved. First, to satisfy the huge demand for electrodes, mass production of high-quality graphene is still challenging. Then, introduction of essential functional groups and surface modification during the device fabrication still require long and arduous processes. In addition, developing easy and effective device fabrication methods towards miniaturized, integrated, and multifunctional devices is still a great challenge. What is more, exploring new materials and electrolyte factors should also be taken into account. Finally, laser processing efficiency should be considered for practical applications. To address this limitation, spatial light modulators and concurrent processing technologies have been widely used to improve processing efficiency. In short, the development of laser-enabled G-SCs may stimulate rapid progress in various wearable devices for future applications.

To summarize, laser-enabled G-SCs are still a promising method for developing high-performance energy storage devices. The method combines advanced fabrication technologies with unique material properties that will stimulate the rapid progress of wearable devices.

Funding. National Key Research and Development Program of China (2017YFB1104600); National Natural Science Foundation of China (61935008, 61775078, 61905087, 61590930); Scientific and Technological Developing Scheme of Jilin Province (20180101061JC).

Disclosures. The authors declare no conflicts of interest.

REFERENCES

1. J. Wu, H. Wang, Z. Su, M. Zhang, X. Hu, Y. Wang, Z. Wang, B. Zhong, W. Zhou, J. Liu, and S. G. Xing, "Highly flexible and sensitive wearable E-skin based on graphite nanoplatelet and polyurethane nanocomposite films in mass industry production available," ACS Appl. Mater. Interfaces **9**, 38745–38754 (2017).
2. Y. Liu, M. Pharr, and G. A. Salvatore, "Lab-on-skin: a review of flexible and stretchable electronics for wearable health monitoring," ACS Nano **11**, 9614–9635 (2017).
3. S. Wang, J. Xu, W. Wang, G. J. N. Wang, R. Rastak, F. Molina-Lopez, J. W. Chung, S. Niu, V. R. Feig, J. Lopez, T. Lei, S. K. Kwon, Y. Kim, A. M. Foudeh, A. Ehrlich, A. Gasperini, Y. Yun, B. Murmann, J. B. H. Tok, and Z. Bao, "Skin electronics from scalable fabrication of an intrinsically stretchable transistor array," Nature **555**, 83–88 (2018).
4. J. N. Wang, Y. Q. Liu, Y. L. Zhang, J. Feng, H. Wang, Y. H. Yu, and H. B. Sun, "Wearable superhydrophobic elastomer skin with switchable wettability," Adv. Funct. Mater. **28**, 1800625 (2018).
5. J. Wu, Z. Ma, Z. Hao, J. T. Zhang, P. Sun, M. Zhang, Y. Liu, Y. Cheng, Y. Li, B. Zhong, T. Zhang, L. Xia, W. Yao, X. Huang, H. Wang, H. Liu, F. Yan, C. E. Hsu, and G. Xing, "Sheath-core fiber strain sensors driven by in-situ crack and elastic effects in graphite nanoplate composites," ACS Appl. Nano Mater. **2**, 750–759 (2019).
6. S. Yao, P. Swetha, and Y. Zhu, "Nanomaterial-enabled wearable sensors for healthcare," Adv. Healthcare Mater. **7**, 1700889 (2018).
7. S. Choi, S. I. Han, D. Jung, H. J. Hwang, C. Lim, S. Bae, O. K. Park, C. M. Tschabrunn, M. Lee, S. Y. Bae, J. W. Yu, J. H. Ryu, S. W. Lee, K. Park, P. M. Kang, W. B. Lee, R. Nezafat, T. Hyeon, and D. H. Kim, "Highly conductive, stretchable and biocompatible Ag-Au core-sheath nanowire composite for wearable and implantable bioelectronics," Nat. Nanotechnol. **13**, 1048–1056 (2018).
8. Y. Yang and W. Gao, "Wearable and flexible electronics for continuous molecular monitoring," Chem. Soc. Rev. **48**, 1465–1491 (2019).
9. M. D. Dickey, "Stretchable and soft electronics using liquid metals," Adv. Mater. **29**, 1606425 (2017).
10. D. Wang, Y. Zhang, X. Lu, Z. Ma, C. Xie, and Z. Zheng, "Chemical formation of soft metal electrodes for flexible and wearable electronics," Chem. Soc. Rev. **47**, 4611–4641 (2018).
11. R. Huang and X. Zhu, "Electrostatic actuating bendable flat electrode for micro electrochemical machining," Nanotechnol. Precis. Eng. **1**, 133–137 (2018).
12. M. Zhang, H. Wang, Z. Su, C. Tian, J. T. Zhang, Y. Wang, F. Yan, Z. Mai, and G. Xing, "Enhanced thermal conductivity and lower density composites with brick-wall microstructure based on highly oriented graphite nanoplatelet: towards manufacturable cooling substrates for high power density electronic devices," Nanotechnology **30**, 245204 (2019).
13. Z. Lu, G. Zhou, M. Song, D. Wang, P. Huo, W. Fan, H. Dong, H. Tang, F. Yan, and G. Xing, "Magnetic functional heterojunction reactors with 3D specific recognition for selective photocatalysis and synergistic photodegradation in binary antibiotic solutions," J. Mater. Chem. A **7**, 13986–14000 (2019).
14. Z. Lu, F. He, C. Y. Hsieh, X. Wu, M. Song, X. Liu, Y. Liu, S. Yuan, H. Dong, S. Han, P. Du, and G. Xing, "Magnetic hierarchical photocatalytic nanoreactors: toward highly selective Cd^{2+} removal with secondary pollution free tetracycline degradation," ACS Appl. Nano Mater. **2**, 1664–1674 (2019).

15. B. Han, Y. L. Zhang, L. Zhu, Y. Li, Z. C. Ma, Y. Q. Liu, X. L. Zhang, X. W. Cao, Q. D. Chen, C. W. Qiu, and H. B. Sun, "Plasmonic-assisted graphene oxide artificial muscles," Adv. Mater. **31**, 245204 (2019).
16. D. Yin, N. R. Jiang, Y. F. Liu, X. L. Zhang, A. W. Li, J. Feng, and H. B. Sun, "Mechanically robust stretchable organic optoelectronic devices built using a simple and universal stencil-pattern transferring technology," Light Sci. Appl. **7**, 35 (2018).
17. Y. L. Zhang, J. N. Ma, S. Liu, D. D. Han, Y. Q. Liu, Z. D. Chen, J. W. Mao, and H. B. Sun, "A "Yin"-"Yang" complementarity strategy for design and fabrication of dual-responsive bimorph actuators," Nano Energy **68**, 104302 (2020).
18. Z. Liu, H. Li, M. Zhu, Y. Huang, Z. Tang, Z. Pei, Z. Wang, Z. Shi, J. Liu, Y. Huang, and C. Zhi, "Towards wearable electronic devices: a quasi-solid-state aqueous lithium-ion battery with outstanding stability, flexibility, safety and breathability," Nano Energy **44**, 164–173 (2018).
19. Y. Huang, W. S. Ip, Y. Y. Lau, J. Sun, J. Zeng, N. S. S. Yeung, W. S. Ng, H. Li, Z. Pei, Q. Xue, Y. Wang, J. Yu, H. Hu, and C. Zhi, "Weavable, conductive yarn-based NiCo//Zn textile battery with high energy density and rate capability," ACS Nano **11**, 8953–8961 (2017).
20. H. Li, C. Han, Y. Huang, Y. Huang, M. Zhu, Z. Pei, Q. Xue, Z. Wang, Z. Liu, Z. Tang, Y. Wang, F. Kang, B. Li, and C. Zhi, "An extremely safe and wearable solid-state zinc ion battery based on a hierarchical structured polymer electrolyte," Energy Environ. Sci. **11**, 941–951 (2018).
21. S. Yun, Y. Qin, A. R. Uhl, N. Vlachopoulos, M. Yin, D. Li, X. Han, and A. Hagfeldt, "New-generation integrated devices based on dye-sensitized and perovskite solar cells," Energy Environ. Sci. **11**, 476–526 (2018).
22. L. Ma, W. Zhang, L. Wang, Y. Hu, G. Zhu, Y. Wang, R. Chen, T. Chen, Z. Tie, J. Liu, and Z. Jin, "Strong capillarity, chemisorption, and electrocatalytic capability of crisscrossed nanostraws enabled flexible, high-rate, and long-cycling lithium sulfur batteries," ACS Nano **12**, 4868–4876 (2018).
23. H. Hou, Q. Xu, Y. Pang, L. Li, J. Wang, C. Zhang, and C. Sun, "Efficient storing energy harvested by triboelectric nanogenerators using a safe and durable all-solid-state sodium-ion battery," Adv. Sci. **4**, 1700072 (2017).
24. H. Long, W. Zeng, H. Wang, M. Qian, Y. Liang, and Z. Wang, "Self-assembled biomolecular 1D nanostructures for aqueous sodium-ion battery," Adv. Sci. **5**, 1700634 (2018).
25. W. S. B. Dwandaru, L. D. Parwati, and R. I. Wisnuwijaya, "Formation of graphene oxide from carbon rods of zinc-carbon battery wastes by audiosonic sonication assisted by commercial detergent," Nanotechnol. Precis. Eng. **2**, 89–94 (2018).
26. R. You, Y. Q. Liu, Y. L. Hao, D. D. Han, Y. L. Zhang, and Z. You, "Laser fabrication of graphene-based flexible electronics," Adv. Mater. 1901981 (2019).
27. C. Wang, C. Wang, Z. Huang, and S. Xu, "Materials and structures toward soft electronics," Adv. Mater. **30**, 1801368 (2018).
28. X. Pu, W. Hu, and Z. L. Wang, "Toward wearable self-charging power systems: the integration of energy-harvesting and storage devices," Small **14**, 1702817 (2018).
29. Y. Ko, M. Kwon, W. K. Bae, B. Lee, S. W. Lee, and J. Cho, "Flexible supercapacitor electrodes based on real metal-like cellulose papers," Nat. Commun. **8**, 536 (2017).
30. J. Lao, P. Sun, F. Liu, X. Zhang, C. Zhao, W. Mai, T. Guo, G. Xiao, and J. Albert, "*In situ* plasmonic optical fiber detection of the state of charge of supercapacitors for renewable energy storage," Light Sci. Appl. **7**, 34 (2018).
31. Z. Wang, H. Wang, Z. Hao, Z. Ma, H. Liu, M. Zhang, Y. Cheng, J. Wu, B. Zhong, L. Xia, W. Yao, W. Zhou, T. Zhang, P. Sun, and S. G. Xing, "Tailoring highly flexible hybrid supercapacitors developed by graphite nanoplatelets-based film: toward integrated wearable energy platform building blocks," ACS Appl. Energy Mater. **1**, 5336–5346 (2018).
32. D. P. Dubal, N. R. Chodankar, D.-H. Kim, and P. Gomez-Romero, "Towards flexible solid-state supercapacitors for smart and wearable electronics," Chem. Soc. Rev. **47**, 2065–2129 (2018).
33. Y. Wang, W. Lai, N. Wang, Z. Jiang, X. Wang, P. Zou, Z. Lin, H. J. Fan, F. Kang, C.-P. Wong, and C. Yang, "A reduced graphene oxide/mixed-valence manganese oxide composite electrode for tailorable and surface mountable supercapacitors with high capacitance and super-long life," Energy Environ. Sci. **10**, 941–949 (2017).
34. N. A. Kyerematen, T. Brousse, and D. Pech, "Microsupercapacitors as miniaturized energy-storage components for on-chip electronics," Nat. Nanotechnol. **12**, 7–15 (2017).
35. Q. Jiang, C. Wu, Z. Wang, A. C. Wang, J.-H. He, Z. L. Wang, and H. N. Alshareef, "MXene electrochemical microsupercapacitor integrated with triboelectric nanogenerator as a wearable self-charging power unit," Nano Energy **45**, 266–272 (2018).
36. W. Raza, F. Ali, N. Raza, Y. Luo, K.-H. Kim, J. Yang, S. Kumar, A. Mehmood, and E. E. Kwon, "Recent advancements in supercapacitor technology," Nano Energy **52**, 441–473 (2018).
37. C. Zhang, M. P. Kremer, A. Seral-Ascaso, S. H. Park, N. McEvoy, B. Anasori, Y. Gogotsi, and V. Nicolosi, "Stamping of flexible, coplanar micro-supercapacitors using MXene inks," Adv. Funct. Mater. **28**, 1705506 (2018).
38. Y. Yang, Q. Huang, L. Niu, D. Wang, C. Yan, Y. She, and Z. Zheng, "Waterproof, ultrahigh areal-capacitance, wearable supercapacitor fabrics," Adv. Mater. **29**, 1606679 (2017).
39. P. Li, Z. Jin, L. Peng, F. Zhao, D. Xiao, Y. Jin, and G. Yu, "Stretchable all-gel-state fiber-shaped supercapacitors enabled by macromolecularly interconnected 3D graphene/nanostructured conductive polymer hydrogels," Adv. Mater. **30**, 1800124 (2018).
40. C. Zhang, B. Anasori, A. Seral-Ascaso, S. H. Park, N. McEvoy, A. Shmeliov, G. S. Duesberg, J. N. Coleman, Y. Gogotsi, and V. Nicolosi, "Transparent, flexible, and conductive 2D titanium carbide (MXene) films with high volumetric capacitance," Adv. Mater. **29**, 1702678 (2017).
41. J. Xu, Y. Sun, M. Lu, L. Wang, J. Zhang, and X. Liu, "One-step electrodeposition fabrication of Ni_3S_2 nanosheet arrays on Ni foam as an advanced electrode for asymmetric supercapacitors," Sci. China Mater. **62**, 699–710 (2019).
42. X. Fu, Z. Li, L. Xu, M. Liao, H. Sun, S. Xie, X. Sun, B. Wang, and H. Peng, "Amphiphilic core-sheath structured composite fiber for comprehensively performed supercapacitor," Sci. China Mater. **62**, 955–964 (2019).
43. P. Kang, K. H. Kim, H. G. Park, and S. Nam, "Mechanically reconfigurable architectured graphene for tunable plasmonic resonances," Light Sci. Appl. **7**, 17 (2018).
44. B. Zeng, Z. Huang, A. Singh, Y. Yao, A. K. Azad, A. D. Mohite, A. J. Taylor, D. R. Smith, and H. T. Chen, "Hybrid graphene metasurfaces for high-speed mid-infrared light modulation and single-pixel imaging," Light Sci. Appl. **7**, 51 (2018).
45. X. Y. Zhang, S. H. Sun, X. J. Sun, Y. R. Zhao, L. Chen, Y. Yang, W. Lu, and D. B. Li, "Plasma-induced, nitrogen-doped graphene-based aerogels for high-performance supercapacitors," Light Sci. Appl. **5**, e16130 (2016).
46. Y. Q. Liu, Z. D. Chen, J. W. Mao, D. D. Han, and X. Sun, "Laser fabrication of graphene-based electronic skin," Front. Chem. **7**, 461 (2019).
47. W. H. Wang, R. X. Du, X. T. Guo, J. Jiang, W. W. Zhao, Z. H. Ni, X. R. Wang, Y. M. You, and Z. H. Ni, "Interfacial amplification for graphene-based position-sensitive-detectors," Light Sci. Appl. **6**, e17113 (2017).
48. Y. L. Shao, M. F. El-Kady, L. J. Wang, Q. H. Zhang, Y. G. Li, H. Z. Wang, M. F. Mousavi, and R. B. Kaner, "Graphene-based materials for flexible supercapacitors," Chem. Soc. Rev. **44**, 3639–3665 (2015).
49. W. K. Chee, H. N. Lim, Z. Zainal, N. M. Huang, I. Harrison, and Y. Andou, "Flexible graphene-based supercapacitors: a review," J. Phys. Chem. C **120**, 4153–4172 (2016).
50. G. P. Xiong, C. Z. Meng, R. G. Reifenberger, P. P. Irazoqui, and T. S. Fisher, "A review of graphene-based electrochemical microsupercapacitors," Electroanalysis **26**, 30–51 (2014).
51. Y. L. Zhang, L. Guo, H. Xia, Q. D. Chen, J. Feng, and H. B. Sun, "Photoreduction of graphene oxides: methods, properties, and applications," Adv. Opt. Mater. **2**, 10–28 (2014).

52. L. Huang, Y. Liu, L. C. Ji, Y. Q. Xie, T. Wang, and W. Z. Shi, "Pulsed laser assisted reduction of graphene oxide," Carbon **49**, 2431–2436 (2011).
53. H. M. Jeong, J. W. Lee, W. H. Shin, Y. J. Choi, H. J. Shin, J. K. Kang, and J. W. Choi, "Nitrogen-doped graphene for high-performance ultracapacitors and the importance of nitrogen-doped sites at basal planes," Nano Lett. **11**, 2472–2477 (2011).
54. R. Ye, D. K. James, and J. M. Tour, "Laser-induced graphene: from discovery to translation," Adv. Mater. **31**, 180362 (2019).
55. Y. L. Zhang, Y. Tian, H. Wang, Z. C. Ma, D. D. Han, L. G. Niu, Q. D. Chen, and H. B. Sun, "Dual-3D femtosecond laser nanofabrication enables dynamic actuation," ACS Nano **13**, 4041–4048 (2019).
56. H. B. Jiang, Y. L. Zhang, D. D. Han, H. Xia, J. Feng, Q. D. Chen, Z. R. Hong, and H. B. Sun, "Bioinspired fabrication of superhydrophobic graphene films by two-beam laser interference," Adv. Funct. Mater. **24**, 4595–4602 (2014).
57. X. Zang, C. Shen, Y. Chu, B. Li, M. Wei, J. Zhong, M. Sanghadasa, and L. Lin, "Laser-induced molybdenum carbide-graphene composites for 3D foldable paper electronics," Adv. Mater. **30**, 1800062 (2018).
58. L. Guo, Y. L. Zhang, D. D. Han, H. B. Jiang, D. Wang, X. B. Li, H. Xia, J. Feng, Q. D. Chen, and H. B. Sun, "Laser-mediated programmable N doping and simultaneous reduction of graphene oxides," Adv. Opt. Mater. **2**, 120–125 (2014).
59. J. Ye, H. Tan, S. Wu, K. Ni, F. Pan, J. Liu, Z. Tao, Y. Qu, H. Ji, P. Simon, and Y. Zhu, "Direct laser writing of graphene made from chemical vapor deposition for flexible, integratable micro-supercapacitors with ultrahigh power output," Adv. Mater. **30**, 1801384 (2018).
60. A. Lamberti, F. Clerici, M. Fontana, and L. Scaltrito, "A highly stretchable supercapacitor using laser-induced graphene electrodes onto elastomeric substrate," Adv. Energy Mater. **6**, 1600050 (2016).
61. D. Shen, G. Zou, L. Liu, W. Zhao, A. Wu, W. W. Duley, and Y. N. Zhou, "Scalable high-performance ultraminiature graphene micro-supercapacitors by a hybrid technique combining direct writing and controllable microdroplet transfer," ACS Appl. Mater. Interfaces **10**, 5404–5412 (2018).
62. Y. Wang, Y. Song, and Y. Xia, "Electrochemical capacitors: mechanism, materials, systems, characterization and applications," Chem. Soc. Rev. **45**, 5925–5950 (2016).
63. P. Simon, Y. Gogotsi, and B. Dunn, "Where do batteries end and supercapacitors begin?" Science **343**, 1210–1211 (2014).
64. X. L. Chen, R. Paul, and L. M. Dai, "Carbon-based supercapacitors for efficient energy storage," Natl. Sci. Rev. **4**, 453–489 (2017).
65. Y. L. Zhang, Y. Q. Liu, D. D. Han, J. N. Ma, D. Wang, X. B. Li, and H. B. Sun, "Quantum-confined-superfluidics-enabled moisture actuation based on unilaterally structured graphene oxide papers," Adv. Mater. **31**, 1901585 (2019).
66. R. You, D. D. Han, F. Liu, Y. L. Zhang, and G. Lu, "Fabrication of flexible room-temperature NO_2 sensors by direct laser writing of In_2O_3 and graphene oxide composites," Sens. Actuators B **277**, 114–120 (2018).
67. B. Senyuk, N. Behabtu, A. Martinez, T. Lee, D. E. Tsentalovich, G. Ceriotti, J. M. Tour, M. Pasquali, and I. I. Smalyukh, "Three-dimensional patterning of solid microstructures through laser reduction of colloidal graphene oxide in liquid-crystalline dispersions," Nat. Commun. **6**, 7157 (2015).
68. D. D. Han, Y. L. Zhang, Y. Liu, Y. Q. Liu, H. B. Jiang, B. Han, X. Y. Fu, H. Ding, H. L. Xu, and H. B. Sun, "Bioinspired graphene actuators prepared by unilateral UV irradiation of graphene oxide papers," Adv. Funct. Mater. **25**, 4548–4557 (2015).
69. D. D. Han, Y. Q. Liu, J. N. Ma, J. W. Mao, Z. D. Chen, Y. L. Zhang, and H. B. Sun, "Biomimetic graphene actuators enabled by multiresponse graphene oxide paper with pretailored reduction gradient," Adv. Mater. Technol. **3**, 1800258 (2018).
70. A. Chaichi, Y. Wang, and M. R. Gartia, "Substrate engineered interconnected graphene electrodes with ultrahigh energy and power densities for energy storage applications," ACS Appl. Mater. Interfaces **10**, 21235–21245 (2018).
71. D. D. Han, Y. L. Zhang, H. B. Jiang, H. Xia, J. Feng, Q. D. Chen, H. L. Xu, and H. B. Sun, "Moisture-responsive graphene paper prepared by self-controlled photoreduction," Adv. Mater. **27**, 332–338 (2015).
72. D. D. Han, Y. L. Zhang, J. N. Ma, Y. Liu, J. W. Mao, C. H. Han, K. Jiang, H. R. Zhao, T. Zhang, H. L. Xu, and H. B. Sun, "Sunlight-reduced graphene oxides as sensitive moisture sensors for smart device design," Adv. Mater. Technol. **2**, 1700045 (2017).
73. V. A. Smirnov, A. A. Arbuzov, Y. M. Shul'ga, S. A. Baskakov, V. M. Martynenko, V. E. Muradyan, and E. I. Kresova, "Photoreduction of graphite oxide," High Energy Chem. **45**, 57–61 (2011).
74. H. B. Jiang, B. Zhao, Y. Liu, S. Y. Li, J. Liu, Y. Y. Song, D. D. Wang, W. Xin, and L. Q. Ren, "Review of photoreduction and synchronous patterning of graphene oxide toward advanced applications," J. Mater. Sci. **55**, 480–497 (2020).
75. R. Arul, R. N. Oosterbeek, J. Robertson, G. Y. Xu, J. Y. Jin, and M. C. Simpson, "The mechanism of direct laser writing of graphene features into graphene oxide films involves photoreduction and thermally assisted structural rearrangement," Carbon **99**, 423–431 (2016).
76. V. A. Smirnov, N. N. Denisov, V. G. Plotnikov, and M. V. Alfimov, "Photochemical processes in graphene oxide films," High Energy Chem. **50**, 51–59 (2016).
77. Y. Q. Liu, J. W. Mao, Z. D. Chen, D. D. Han, Z. Z. Jiao, J. N. Ma, H. B. Jiang, and H. Yang, "Three-dimensional micropatterning of graphene by femtosecond laser direct writing technology," Opt. Lett. **45**, 113–116 (2020).
78. Y. Zhang, L. Guo, S. Wei, Y. He, H. Xia, Q. Chen, H. B. Sun, and F. S. Xiao, "Direct imprinting of microcircuits on graphene oxides film by femtosecond laser reduction," Nano Today **5**, 15–20 (2010).
79. D. D. Han, Y. L. Zhang, J. N. Ma, Y. Q. Liu, B. Han, and H. B. Sun, "Light-mediated manufacture and manipulation of actuators," Adv. Mater. **28**, 8328–8343 (2016).
80. H. B. Jiang, Y. Liu, J. Liu, S. Y. Li, Y. Y. Song, D. D. Han, and L. Q. Ran, "Moisture-responsive graphene actuators prepared by two-beam laser interference of graphene oxide paper," Front. Chem. **7**, 464 (2019).
81. C. Ogata, R. Kurogi, K. Awaya, K. Hatakeyama, T. Taniguchi, M. Koinuma, and Y. Matsumoto, "All-graphene oxide flexible solid-state supercapacitors with enhanced electrochemical performance," ACS Appl. Mater. Interfaces **9**, 26151–26160 (2017).
82. S. Wang, Z.-S. Wu, S. Zheng, F. Zhou, C. Sun, H. M. Cheng, and X. Bao, "Scalable fabrication of photochemically reduced graphene-based monolithic micro-supercapacitors with superior energy and power densities," ACS Nano **11**, 4283–4291 (2017).
83. V. Strauss, K. Marsh, M. D. Kowal, M. El-Kady, and R. B. Kaner, "A simple route to porous graphene from carbon nanodots for supercapacitor applications," Adv. Mater. **30**, 1704449 (2018).
84. V. Strauss, M. Anderson, C. Wang, A. Borenstein, and R. B. Kaner, "Carbon nanodots as feedstock for a uniform hematite-graphene nanocomposite," Small **14**, 1803656 (2018).
85. L. B. Xing, S. F. Hou, J. Zhou, S. Li, T. Zhu, Z. Li, W. Si, and S. Zhuo, "UV-assisted photoreduction of graphene oxide into hydrogels: high-rate capacitive performance in supercapacitor," J. Phys. Chem. C **118**, 25924–25930 (2014).
86. H. Huang, C. Lei, G. Luo, G. Li, X. Liang, S. Tang, and Y. Du, "UV-assisted reduction of graphene oxide on Ni foam as high performance electrode for supercapacitors," Carbon **107**, 917–924 (2016).
87. W. Gao, N. Singh, L. Song, Z. Liu, A. L. M. Reddy, L. Ci, R. Vajtai, Q. Zhang, B. Wei, and P. M. Ajayan, "Direct laser writing of micro-supercapacitors on hydrated graphite oxide films," Nat. Nanotechnol. **6**, 496–500 (2011).
88. Q. Pan, N. Tong, N. He, Y. Liu, E. Shim, B. Pourdeyhimi, and W. Gao, "Electrospun mat of poly(vinyl alcohol)/graphene oxide for superior electrolyte performance," ACS Appl. Mater. Interfaces **10**, 7927–7934 (2018).
89. Y. Hu, H. Cheng, F. Zhao, N. Chen, L. Jiang, Z. Feng, and L. Qu, "All-in-one graphene fiber supercapacitor," Nanoscale **6**, 6448–6451 (2014).
90. M. F. El-Kady and R. B. Kaner, "Scalable fabrication of high-power graphene micro-supercapacitors for flexible and on-chip energy storage," Nat. Commun. **4**, 1475 (2013).

91. M. Wu, Y. Li, B. Yao, J. Chen, C. Li, and G. Shi, "A high-performance current collector-free flexible in-plane micro-supercapacitor based on a highly conductive reduced graphene oxide film," J. Mater. Chem. A **4**, 16213–16218 (2016).
92. Y. Shao, J. Li, Y. Li, H. Wang, Q. Zhang, and R. B. Kaner, "Flexible quasi-solid-state planar micro-supercapacitor based on cellular graphene films," Mater. Horiz. **4**, 1145–1150 (2017).
93. Y. Liu, B. Weng, Q. Xu, Y. Hou, C. Zhao, S. Beirne, K. Shu, R. Jalili, G. G. Wallace, J. M. Razal, and J. Chen, "Facile fabrication of flexible microsupercapacitor with high energy density," Adv. Mater. Technol. **1**, 1600166 (2016).
94. B. Xie, Y. Wang, W. Lai, W. Lin, Z. Lin, Z. Zhang, P. Zou, Y. Xu, S. Zhou, C. Yang, F. Kang, and C.-P. Wong, "Laser-processed graphene based micro-supercapacitors for ultrathin, rollable, compact and designable energy storage components," Nano Energy **26**, 276–285 (2016).
95. J. W. Suk, A. Kitt, C. W. Magnuson, Y. Hao, S. Ahmed, J. An, A. K. Swan, B. B. Goldberg, and R. S. Ruoff, "Transfer of CVD-grown monolayer graphene onto arbitrary substrates," ACS Nano **5**, 6916–6924 (2011).
96. C. Mattevi, H. Kim, and M. Chhowalla, "A review of chemical vapour deposition of graphene on copper," J. Mater. Chem. **21**, 3324–3334 (2011).
97. S. Zhou, J. Xu, Y. Xiao, N. Zhao, and C.-P. Wong, "Low-temperature Ni particle-templated chemical vapor deposition growth of curved graphene for supercapacitor applications," Nano Energy **13**, 458–466 (2015).
98. L. Zheng, X. Cheng, P. Ye, L. Shen, Q. Wang, D. Zhang, Z. Gu, W. Zhou, D. Wua, and Y. Yu, "Low temperature growth of three-dimensional network of graphene for high-performance supercapacitor electrodes," Mater. Lett. **218**, 90–94 (2018).
99. X. Zang, P. Li, Q. Chen, K. Wang, J. Wei, D. Wu, and H. Zhu, "Evaluation of layer-by-layer graphene structures as supercapacitor electrode materials," J. Appl. Phys. **115**, 024305 (2014).
100. P. Xu, J. Kang, J. B. Choi, J. Suhr, J. Yu, F. Li, J. H. Byun, B. S. Kim, and T. W. Chou, "Laminated ultrathin chemical vapor deposition graphene films based stretchable and transparent high-rate supercapacitor," ACS Nano **8**, 9437–9445 (2014).
101. J. Lin, Z. Peng, Y. Liu, F. Ruiz-Zepeda, R. Ye, E. L. G. Samuel, M. J. Yacaman, B. I. Yakobson, and J. M. Tour, "Laser-induced porous graphene films from commercial polymers," Nat. Commun. **5**, 5714 (2014).
102. Z. Peng, J. Lin, R. Ye, E. L. G. Samuel, and J. M. Tour, "Flexible and stackable laser-induced graphene supercapacitors," ACS Appl. Mater. Interfaces **7**, 3414–3419 (2015).
103. R. Ye, Y. Chyan, J. Zhang, Y. Li, X. Han, C. Kittrell, and J. M. Tour, "Laser-induced graphene formation on wood," Adv. Mater. **29**, 1702211 (2017).
104. Y. Chyan, R. Ye, Y. Li, S. P. Singh, C. J. Arnusch, and J. M. Tour, "Laser-induced graphene by multiple lasing: toward electronics on cloth, paper, and food," ACS Nano **12**, 2176–2183 (2018).
105. A. Lamberti, M. Serrapede, G. Ferraro, M. Fontana, F. Perrucci, S. Bianco, A. Chiolerio, and S. Bocchini, "All-SPEEK flexible supercapacitor exploiting laser-induced graphenization," 2D Mater. **4**, 035012 (2017).
106. M. F. El-Kady, V. Strong, S. Dubin, and R. B. Kaner, "Laser scribing of high-performance and flexible graphene-based electrochemical capacitors," Science **335**, 1326–1330 (2012).
107. X. Y. Fu, Y. L. Zhang, H. B. Jiang, D. D. Han, Y. Q. Liu, H. Xia, and H. B. Sun, "Hierarchically structuring and synchronous photoreduction of graphene oxide films by laser holography for supercapacitors," Opt. Lett. **44**, 1714–1717 (2019).
108. X. Y. Fu, Z. D. Chen, Y. L. Zhang, D. D. Han, J. N. Ma, W. Wang, Z. R. Zhang, H. Xia, and H. B. Sun, "Direct laser writing of flexible planar supercapacitors based on GO and black phosphorus quantum dot nanocomposites," Nanoscale **11**, 9133–9140 (2019).
109. A. Perez del Pino, A. Martinez Villarroya, A. Chuquitarqui, C. Logofatu, D. Tonti, and E. Gyorgy, "Reactive laser synthesis of nitrogen-doped hybrid graphene-based electrodes for energy storage," J. Mater. Chem. A **6**, 16074–16086 (2018).
110. G. W. Huang, N. Li, Y. Du, Q. P. Feng, H. M. Xiao, X. H. Wu, and S. Y. Fu, "Laser-printed in-plane micro-supercapacitors: from symmetric to asymmetric structure," ACS Appl. Mater. Interfaces **10**, 723–732 (2018).
111. F. Wen, C. Hao, J. Xiang, L. Wang, H. Hou, Z. Su, W. Hu, and Z. Liu, "Enhanced laser scribed flexible graphene-based micro-supercapacitor performance with reduction of carbon nanotubes diameter," Carbon **75**, 236–243 (2014).
112. R. Z. Li, R. Peng, K. D. Kihm, S. Bai, D. Bridges, U. Tumuluri, Z. Wu, T. Zhang, G. Compagnini, Z. Feng, and A. Hu, "High-rate in-plane micro-supercapacitors scribed onto photo paper using in situ femtolaser-reduced graphene oxide/Au nanoparticle microelectrodes," Energy Environ. Sci. **9**, 1458–1467 (2016).
113. J. Y. Hwang, M. F. El-Kady, Y. Wang, L. Wang, Y. Shao, K. Marsh, J. M. Ko, and R. B. Kaner, "Direct preparation and processing of graphene/RuO_2 nanocomposite electrodes for high-performance capacitive energy storage," Nano Energy **18**, 57–70 (2015).
114. J. Y. Hwang, M. F. El-Kady, M. Li, C. W. Lin, M. Kowal, X. Han, and R. B. Kaner, "Boosting the capacitance and voltage of aqueous supercapacitors via redox charge contribution from both electrode and electrolyte," Nano Today **15**, 15–25 (2017).
115. F. Clerici, M. Fontana, S. Bianco, M. Serrapede, F. Perrucci, S. Ferrero, E. Tresso, and A. Lamberti, "In situ MoS_2 decoration of laser-induced graphene as flexible supercapacitor electrodes," ACS Appl. Mater. Interfaces **8**, 10459–10465 (2016).
116. E. Ghoniem, S. Mori, and A. Abdel-Moniem, "Low-cost flexible supercapacitors based on laser reduced graphene oxide supported on polyethylene terephthalate substrate," J. Power Sources **324**, 272–281 (2016).
117. L. Li, J. Zhang, Z. Peng, Y. Li, C. Gao, Y. Ji, R. Ye, N. D. Kim, Q. Zhong, Y. Yang, H. Fei, G. Ruan, and J. M. Tour, "High-performance pseudocapacitive microsupercapacitors from laser-induced graphene," Adv. Mater. **28**, 838–845 (2016).
118. Z. Peng, R. Ye, J. A. Mann, D. Zakhidov, Y. Li, P. R. Smalley, J. Lin, and J. M. Tour, "Flexible boron-doped laser-induced graphene microsupercapacitors," ACS Nano **9**, 5868–5875 (2015).
119. S. Park, H. Lee, Y. J. Kim, and P. S. Lee, "Fully laser-patterned stretchable microsupercapacitors integrated with soft electronic circuit components," NPG Asia Mater. **10**, 959–969 (2018).
120. Z. Wen, X. Wang, S. Mao, Z. Bo, H. Kim, S. Cui, G. Lu, X. Feng, and J. Chen, "Crumpled nitrogen-doped graphene nanosheets with ultrahigh pore volume for high-performance supercapacitor," Adv. Mater. **24**, 5610–5616 (2012).
121. Y. Zhao, C. Hu, Y. Hu, H. Cheng, G. Shi, and L. Qu, "A versatile, ultralight, nitrogen-doped graphene framework," Angew. Chem. (Int. Ed.) **51**, 11371–11375 (2012).
122. Z. Lei, L. Lu, and X. S. Zhao, "The electrocapacitive properties of graphene oxide reduced by urea," Energy Environ. Sci. **5**, 6391–6399 (2012).
123. H. C. Youn, S. M. Bak, M. S. Kim, C. Jaye, D. A. Fischer, C. W. Lee, X. Q. Yang, K. C. Roh, and K. B. Kim, "High-surface-area nitrogen-doped reduced graphene oxide for electric double-layer capacitors," ChemSusChem **8**, 1875–1884 (2015).
124. A. L. M. Reddy, A. Srivastava, S. R. Gowda, H. Gullapalli, M. Dubey, and P. M. Ajayan, "Synthesis of nitrogen-doped graphene films for lithium battery application," ACS Nano **4**, 6337–6342 (2010).
125. S. P. Singh, Y. Li, J. Zhang, J. M. Tour, and C. J. Arnusch, "Sulfur-doped laser-induced porous graphene derived from polysulfone-class polymers and membranes," ACS Nano **12**, 289–297 (2018).
126. X.-Y. Fu, D.-L. Chen, Y. Liu, H.-B. Jiang, H. Xia, H. Ding, and Y.-L. Zhang, "Laser reduction of nitrogen-rich carbon nanoparticles@graphene oxides composites for high rate performance supercapacitors," ACS Appl. Nano Mater. **1**, 777–784 (2018).
127. F. Wang, X. Dong, K. Wang, W. Duan, M. Gao, Z. Zhai, C. Zhu, and W. Wang, "Laser-induced nitrogen-doped hierarchically porous graphene for advanced electrochemical energy storage," Carbon **150**, 396–407 (2019).
128. D. E. Lobo, P. C. Banerjee, C. D. Easton, and M. Majumder, "Miniaturized supercapacitors: focused ion beam reduced graphene

oxide supercapacitors with enhanced performance metrics," Adv. Energy Mater. **5**, 1500665 (2015).
129. C. Shao, T. Xu, J. Gao, Y. Liang, Y. Zhao, and L. Qu, "Flexible and integrated supercapacitor with tunable energy storage," Nanoscale **9**, 12324–12329 (2017).
130. J. Cai, C. Lv, and A. Watanabe, "Laser direct writing and selective metallization of metallic circuits for integrated wireless devices," ACS Appl. Mater. Interfaces **10**, 915–924 (2018).
131. S. L. Kim, J.-H. Hsu, and C. Yu, "Intercalated graphene oxide for flexible and practically large thermoelectric voltage generation and simultaneous energy storage," Nano Energy **48**, 582–589 (2018).
132. J. Cai, C. Lv, and A. Watanabe, "Laser direct writing of high-performance flexible all-solid-state carbon micro-supercapacitors for an on-chip self-powered photodetection system," Nano Energy **30**, 790–800 (2016).
133. H. Liu, M. Li, R. B. Kaner, S. Chen, and Q. Pei, "Monolithically integrated self-charging power pack consisting of a silicon nanowire array/conductive polymer hybrid solar cell and a laser-scribed graphene supercapacitor," ACS Appl. Mater. Interfaces **10**, 15609–15615 (2018).
134. L. V. Thekkekara, B. Jia, Y. Zhang, L. Qiu, D. Li, and M. Gu, "On-chip energy storage integrated with solar cells using a laser scribed graphene oxide film," Appl. Phys. Lett. **107**, 031105 (2015).